

# Synthesis and Characterization of a New Tiara Pd(II) Thiolate Complex, $[\text{Pd}(\text{SC}_{12}\text{H}_{25})_2]_6$ , and Its Solution-Phase Thermolysis to Prepare Nearly Monodisperse Palladium Sulfide Nanoparticles

Zhiqiang Yang, Alexander B. Smetana, Christopher M. Sorensen, and Kenneth J. Klabunde\*

Departments of Chemistry and Physics, Kansas State University, Manhattan, Kansas 66506

Received July 5, 2006

A new tiara Pd(II) thiolate complex,  $[\text{Pd}(\text{SC}_{12}\text{H}_{25})_2]_6$ , has been synthesized and fully characterized by X-ray single crystal analysis, elemental analysis, MALDI,  $^1\text{H}$  NMR, powder XRD, IR, Raman, and UV/vis. It was found that, in each complex cluster, the six palladium atoms form a nearly planar hexagonal ring and the adjacent palladium atoms are bridged by sulfur atoms from both sides. Then the complex was further used as a single-source precursor to prepare nearly monodisperse palladium sulfide (PdS) nanoparticles through the high-temperature-induced decomposition in diphenyl ether. The obtained nanoparticles are  $2.87 \pm 0.51$  nm in diameter and protected by a layer of thiolate species on the surface.

## Introduction

A variety of metal alkanethiolates have been synthesized and characterized because of their interesting structural features for coordination chemistry and wide applications for monolayer-protected clusters and surface chemistry.

According to their solubility, metal alkanethiolates can be roughly separated into two groups.  $\text{Ag(I)}$ ,<sup>1–3</sup>  $\text{Cu(I)}$ ,<sup>4</sup> and  $\text{Pb(II)}$ <sup>5,6</sup> ions react with primary alkanethiols and form insoluble precipitates in most organic solvents. Through powder XRD analysis, these alkanethiolates show equally separated peaks and can be inferred to have layered structures. On the other hand,  $\text{Ni(II)}$  and  $\text{Pd(II)}$  ions produce soluble cyclic (tiara) compounds with primary alkanethiols or other functionalized thiols. In such structures, every metal ion is coordinated to four sulfur atoms in an approximate square plane and each  $-\text{SR}$  ligand is connected to two metal ions. Depending on the properties of the ligands and the reaction conditions, tiara  $\text{Ni(II)}$  thiolates with 4-, 5-, 6-, 8-, 9-, or 11-membered  $\text{Ni(II)}$  rings have been prepared.<sup>7,8</sup>

Compared to  $\text{Ni(II)}$  thiolates, fewer tiara  $\text{Pd(II)}$  thiolates with short C-chain ligands have been prepared and characterized, including  $[\text{Pd}(\text{SCH}_2\text{CH}_2\text{OH})_2]_6$ ,<sup>9</sup>  $[\text{Pd}(\text{SCH}_2\text{CH}_2\text{CH}_3)_2]_6$ ,<sup>10</sup> and  $[\text{Pd}(\text{SCH}_2\text{CH}_2\text{CH}_3)_2]_8$ .<sup>11</sup> Some theoretical articles described the important role that metal–S  $\pi$  bonds play to stabilize such tiaralike structures.<sup>12–14</sup>

An important application of metal thiolates is to produce metals or metal sulfides through heat-induced decomposition, which can be carried out in solvents with high boiling point or under solventless conditions. Carotenuto et al. reported a general method to synthesize metal or metal sulfide clusters embedded in polymer matrices.<sup>15</sup> Nakamoto et al. presented the thermolysis of a series of gold thiolate precursors  $[\text{RN}(\text{CH}_3)_3][\text{Au}(\text{SC}_{12}\text{H}_{25})_2]$  ( $\text{R} = \text{C}_8\text{H}_{17}$ ,  $\text{C}_{12}\text{H}_{25}$ , and  $\text{C}_{14}\text{H}_{29}$ ) to produce spherical Au nanoparticles.<sup>16,17</sup> Korgel et al. reported the solventless synthesis of nickel sulfide and copper sulfide

\* To whom correspondence should be addressed. Phone: 785-532-6849. Fax: 785-532-6666. E-mail: kenjk@ksu.edu.

- (1) Bensebaa, F.; Ellis, T. H.; Hruus, E.; Voicu, R.; Zhou, Y. *Langmuir* **1998**, *14*, 6579–6587.
- (2) Baena, M. J.; Espinet, P.; Lequerica, M. C.; Levelut, A. M. *J. Am. Chem. Soc.* **1992**, *114*, 4182–4185.
- (3) Dance, I. G.; Fisher, K. J.; Herath Banda, R. M.; Scudder, M. L. *Inorg. Chem.* **1991**, *30*, 183–187.
- (4) Sandhyarani, N.; Predeep, T. *J. Mater. Chem.* **2001**, *11*, 1294–1299.
- (5) Shaw, R. A.; Woods, M. *J. Chem. Soc. A* **1971**, *10*, 1569–1571.
- (6) Tiers, G. V. D.; Brostrom, M. L. *J. Appl. Cryst.* **2000**, *33*, 915–920.

- (7) Woodward, P.; Dahl, L. F.; Abel, E. W.; Crosse, B. C. *J. Am. Chem. Soc.* **1965**, *87*, 5251–5253.
- (8) Ivanov, S. A.; Kozee, M. A.; Merrill, W. A.; Agarwal, S.; Dahl, L. F. *J. Chem. Soc. Dalton Trans.* **2002**, 4105–4115.
- (9) Gould, R. O.; Harding, M. M. *J. Chem. Soc. A* **1970**, 875–881.
- (10) Kunchur, N. R. *Acta Crystallogr.* **1968**, *B24*, 1623–1633.
- (11) Higgins, J. D., III; Suggs, J. W. *Inorg. Chim. Acta* **1988**, *145*, 247–252.
- (12) Nobusada, K.; Yamaki, T. *J. Phys. Chem A* **2004**, *108*, 1813–1817.
- (13) Alemany, P.; Hoffmann, R. *J. Am. Chem. Soc.* **1993**, *115*, 8290–8297.
- (14) Datta, A.; John, N. S.; Kulkarni, G. U.; Pati, S. K. *J. Phys. Chem A* **2005**, *109*, 11647–11649.
- (15) Carotenuto, G.; Martorana, B.; Perlo, P.; Nicolais, L. *J. Mater. Chem.* **2003**, *13*, 2927–2930.
- (16) Nakamoto, M.; Yamamoto, M.; Fukusumi, M. *J. Chem. Soc. Chem. Commun.* **2002**, 1622–1623.

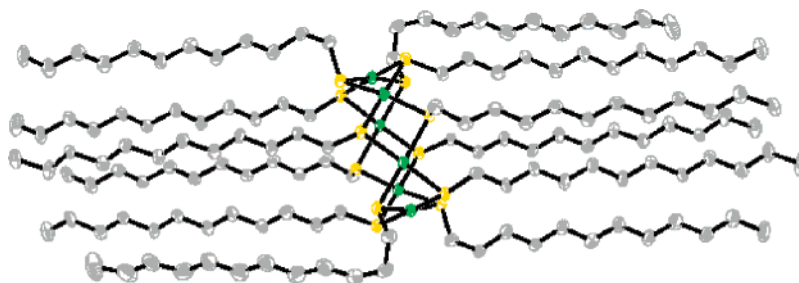


**Figure 1.** Perspective view of the complex  $[\text{Pd}(\text{SC}_{12}\text{H}_{25})_2]_6$ . Yellow balls represent S atoms, while green balls represent Pd atoms.

through the decomposition of the corresponding thiolate precursors in the presence of octanoate.<sup>18,19</sup> Through changing the reaction conditions, nanorods or triangular nanoprisms for NiS and nanorods or spherical nanoparticles for  $\text{Cu}_2\text{S}$  were obtained. Wu et al. reported the synthesis of  $\text{Cu}_2\text{S}$  nanowires<sup>20</sup> and Ag nanodisks<sup>21</sup> through the thermolysis of the respective metal thiolates. Titanium sulfide ( $\text{TiS}_2$ ) and niobium sulfide ( $\text{NbS}_2$ ) thin films have been prepared through chemical vapor deposition by using the corresponding metal *tert*-butylthiolates.<sup>22,23</sup> Recently, copper–indium sulfide nanocrystal heterostructures with interesting shapes were obtained from the thermolysis of a mixture composed of Cu–oleate, In–oleate, and an alkanethiol.<sup>24</sup>

PdS is a semiconductor with an energy gap about 2 eV and has a variety of applications in materials science and catalysis.<sup>25</sup> PdS films have been prepared by laser or thermal vapor deposition from a single-source precursor,  $\text{Pd}(\text{S}_2\text{-COCHMe}_2)_2$ .<sup>26</sup> Yamamoto et al. reported the preparation of PdS organosols through the reaction of Pd acetate with hydrogen sulfide.<sup>27</sup> Also, the first trioctylphosphine oxide (TOPO)-capped PdS nanoparticles have been synthesized through the thermolysis of  $\text{Pd}(\text{S}_2\text{CNMe}(\text{Hex}))_2$  in the presence of TOPO.<sup>28</sup> The tetragonal crystal structure of PdS has been precisely determined by single crystal analysis.<sup>29</sup>

In this paper we report the synthesis and full characterization of a new tiara Pd(II) thiolate complex,  $[\text{Pd}(\text{SC}_{12}\text{H}_{25})_2]_6$ , which was further used as a single-source precursor to prepare nearly monodisperse palladium sulfide (PdS) nano-

particles. This will not only enlarge our understanding about metal thiolate complexes with tiara structures but also offer a novel and facile method to prepare palladium sulfide nanoparticles.

## Experimental Section

**Materials.** Sodium tetrachloropalladate(II) (99%) and 1-dodecanethiol (98%) were obtained from Aldrich Chem. Co. 1-Dodecanethiol (98%), diphenyl ether, and 4-*tert*-butyltoluene (96%) were bought from ACROS Organics. Other chemicals were purchased and used as received.

**Preparation of the Pd(II) Thiolate Complex  $[\text{Pd}(\text{SC}_{12}\text{H}_{25})_2]_6$ .** In a glass tube equipped with a rubber septum which was connected to a vacuum line and an argon gas tank through needles, 0.588 g of  $\text{Na}_2\text{PdCl}_4$  ( $2 \times 10^{-3}$  mol), 10 mL of 4-*tert*-butyltoluene, and 0.98 mL of dodecanethiol ( $4 \times 10^{-3}$  mol) were added sequentially. The mixture was degassed and then flushed with argon several times. Then, it was refluxed (about 192 °C) in a preheated sand bath for 1 h under an atmosphere of argon. After that, the tube was removed from the sand bath and left to cool. The obtained orange-red solution was then dropped into 100 mL of 95% ethanol, which was stirred violently. Orange precipitates and a few red oil droplets formed immediately. Stirring overnight caused the droplets to also form orange precipitates. The final product was separated by centrifugation and washed with 95% ethanol (30 mL  $\times$  4) and then pure ethanol (30 mL  $\times$  4). After being dried at 45 °C under vacuum overnight, 0.93 g of orange powder was obtained. Yield: 91.2%. Anal. Found Pd: 20.56, S: 12.56, C: 56.26, H: 9.42. Calcd Pd: 20.92, S: 12.60, C: 56.65, H: 9.83. For the UV/vis analysis, certain amounts of dry powder were dissolved in *n*-heptane.

**Solution-Phase Thermolysis.** In a glass tube, 0.102 g of the obtained orange powder was added to 4 mL of diphenyl ether. The mixture was degassed and flushed with argon several times. After that, the mixture was refluxed (about 259 °C) in a preheated sand bath for 6 h under the protection of argon. During this process, the original clear orange-red solution became black, which indicated the formation of palladium sulfide nanoparticles. For the UV/vis tracking, the reaction was stopped at different times and cooled to room temperature. Then 16  $\mu\text{L}$  of solution was taken out and mixed with 3 mL of toluene. The UV/vis absorbance was measured using pure toluene as a reference. For TEM analysis, some colloidal solution was taken out and washed with acetone (30 mL  $\times$  4) by centrifugation and then redissolved into 4-*tert*-butyltoluene. For elemental analysis, the washed sample was further dried at 45 °C under vacuum overnight.

**Equipment and Analysis.** UV/vis absorption analysis was carried out on a Cary 500 UV/vis/NIR spectrophotometer. Transmission electron microscopy (TEM) was performed on a Philips CM100 microscopy operated at 100 kV. To prepare a TEM sample, a drop of colloidal solution was dropped onto a carbon-coated

- (17) Nakamoto, M.; Kashiwagi, Y.; Yamamoto, M. *Inorg. Chim. Acta* **2005**, 358, 4229–4236.
- (18) Ghezelbash, A.; Sigman, M. B., Jr.; Korgel, B. A. *Nano Lett.* **2004**, 4, 537–542.
- (19) Larsen, T. H.; Sigman, M. B.; Ghezelbash, A.; Doty, R. C.; Korgel, B. A. *J. Am. Chem. Soc.* **2003**, 125, 5638–5639.
- (20) Chen, L.; Chen, Y. B.; Wu, L. M. *J. Am. Chem. Soc.* **2004**, 126, 16334–16335.
- (21) Chen, Y. B.; Chen, L.; Wu, L. M. *Inorg. Chem.* **2005**, 44, 9817–9822.
- (22) Carmalt, C. J.; O'Neill, S. A.; Parkin, I. P.; Peters, E. S. *J. Mater. Chem.* **2004**, 14, 830–834.
- (23) Carmalt, C. J.; Manning, T. D.; Parkin, I. P.; Peters, E. S.; Hector, A. L. *J. Mater. Chem.* **2004**, 14, 290–291.
- (24) Choi, S. H.; Kim, E. G.; Hyeon, T. *J. Am. Chem. Soc.* **2006**, 128, 2520–2521.
- (25) Dey, S.; Jain, V. K. *Platinum Met. Rev.* **2004**, 48, 16–29.
- (26) Cheon, J.; Talaga, D. S.; Zink, J. I. *Chem. Mater.* **1997**, 9, 1208–1212.
- (27) Yamamoto, T.; Taniguchi, A.; Dev, S.; Osakada, K.; Kubota, K. *Colloid Polym. Sci.* **1991**, 269, 969–971.
- (28) Malik, M. A.; O'Brien, P.; Revaprasadu, N. *J. Mater. Chem.* **2002**, 12, 92–97.
- (29) Brese, N. E.; Squattrito, P. S.; Ibers, J. A. *Acta Crystallogr.* **1985**, C41, 1829–1830.

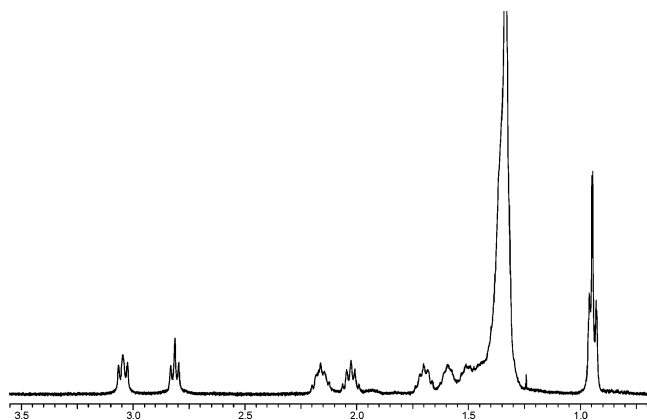
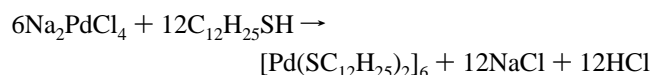


**Figure 2.**  $^1\text{H}$  NMR (room temperature in deuterobenzene) spectrum of  $[\text{Pd}(\text{SC}_{12}\text{H}_{25})_2]_6$ . (3.04 ppm, 12H (t); 2.81 ppm, 12H (t); 2.16 ppm, 12H (q); 2.02 ppm, 12H (q); 1.70–1.34 ppm, 216H (m); 0.94 ppm, 36H (m).)

Formvar copper grid and then allowed to dry in air. IR spectra were obtained using a NEXUS 670 FT-IR system produced by Nicolet Instrument Corporation.  $^1\text{H}$  NMR spectra were obtained on a Varian Unity 400 Plus 400-MHz NMR system. A  $[\text{Pd}(\text{SC}_{12}\text{H}_{25})_2]_6$  single crystal was analyzed through a Bruker SMART 1000 CCD instrument with Mo X-ray irradiation. To obtain the single crystal, product was dissolved in a THF/4-*tert*-butyltoluene mixture (volume ratio: 1/1) and then left uncovered on the bench for several days at room temperature. MALDI mass analysis was performed on an Applied Biosystem DE-Pro MALDI-TOF system. The sample was dissolved in THF and then mixed with 2,5-dihydrobenzoic acid (a matrix) and a cationizing agent ( $\text{CF}_3\text{-COONa}$ ). A positive scan was carried out. Powder XRD patterns were recorded by a Bruker D8 X-ray diffractometer with Cu  $K\alpha$  radiation.

## Results and Discussion

**Preparation of  $[\text{Pd}(\text{SC}_{12}\text{H}_{25})_2]_6$ .** To prepare the Pd(II) thiolate complex,  $\text{Na}_2\text{PdCl}_4$  was used as the Pd(II) source and dodecanethiol as ligand, while 4-*tert*-butyltoluene was applied as a solvent. The reaction is assumed to happen according to the following equation:



When the thiol ligand was added into the suspension of  $\text{Na}_2\text{PdCl}_4$  in 4-*tert*-butyltoluene at room temperature, a white fog formed, which was assumed to be the release of the HCl. In the meantime, the color of the solution changed from colorless to orange-red and part of the brown-colored  $\text{Na}_2\text{-PdCl}_4$  faded into colorless crystals, which indicated the formation of NaCl.

Although this reaction could initiate at room temperature, as described above, it was found not to go to completion unless heated. A control experiment was carried out to show this. When other conditions remained the same, the mixture of the starting materials was stirred at room temperature for 1 h under argon, instead of refluxing. A similar orange powder could be obtained, but more reddish compared with the refluxed sample. Through thin layer chromatography analysis, three products were found for the room-temperature sample, while only one sample point existed for the refluxed

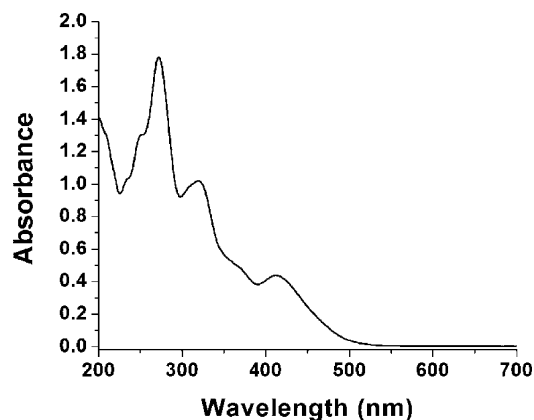


**Figure 3.** UV/vis spectrum of  $[\text{Pd}(\text{SC}_{12}\text{H}_{25})_2]_6$  ( $0.2 \times 10^{-4}$  M in *n*-heptane).

sample (see Supporting Information, Figure S1). These results clearly indicate that without heating, only a mixture can be obtained, which probably contains  $[\text{Pd}(\text{SC}_{12}\text{H}_{25})_2]_6$  and other Pd(II) complexes.

**Structure and Properties of  $[\text{Pd}(\text{SC}_{12}\text{H}_{25})_2]_6$ .** Through single-crystal X-ray analysis, the obtained product was revealed to be a new Pd(II) thiolate complex with a tiara structure. (Figure 1) The crystal was found to be in the  $P\bar{1}$  space group with  $a = 13.2189(14)$  Å,  $b = 18.2919(18)$  Å,  $c = 19.1575(19)$  Å;  $\alpha = 66.529(5)^\circ$ ,  $\beta = 70.892(8)^\circ$ ,  $\gamma = 77.054(7)^\circ$ . In each cluster, the six palladium atoms form a nearly planar hexagonal ring with the average Pd–Pd distance about 3.11 Å. Each palladium atom is coordinated to four sulfur atoms with an approximately square planar geometry, and the average Pd–S bond length is 2.32 Å. The 12 total sulfur atoms form two  $\text{S}_6$  hexagons parallel to the center  $\text{Pd}_6$  ring from both sides. The average S–S distance in each  $\text{S}_6$  ring is 3.50 Å. Such a triple-layered tiara structure is about 3.04 Å in height with a  $D_{6h}$  symmetry (see Supporting Information, Tables S1, S2, and S3 for detailed structural data).

As shown in Figure 1, the S–C bonds are alternately directed either parallel or perpendicular to the  $\text{S}_6$  rings. Such an arrangement is attributed to the steric repulsion and has been found in other  $[\text{Pd}(\text{SR})_2]_6$  or  $[\text{Ni}(\text{SR})_2]_6$  complexes with much shorter substituents.<sup>7–11</sup> The  $^1\text{H}$  NMR spectrum clearly shows this structural feature. (Figure 2)

The two triplets at 3.04 and 2.81 ppm represent the H atoms in  $\text{SCH}_2$  groups. Because of the different orientation, the chemical shift differs by 0.23 ppm. Similar situations occur for H atoms in  $(\text{SCH}_2)\text{CH}_2$  groups, and such differences decrease when the  $\text{CH}_2$  groups are further away from the tiara ring. Also, a high-temperature  $^1\text{H}$  NMR (80 °C) spectrum shows no significant changes in shift, which indicates the relatively stable steric arrangement (see Supporting Information, Figure S2).

As also indicated in Figure 1, all the long chains of the C backbone are packed roughly parallel to each other regardless of the orientation the S–C bonds, so the overall geometry of this cluster is  $C_i$ .

In the UV/vis spectrum, three main peaks (412, 320, 272 nm) and one shoulder peak (248 nm) are observed. (Figure



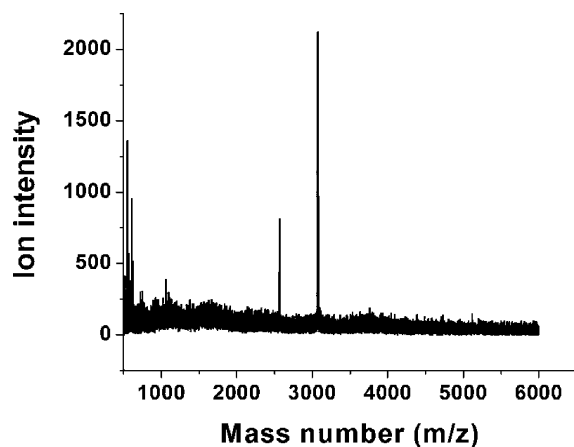


Figure 4. MALDI spectrum of  $[\text{Pd}(\text{SC}_{12}\text{H}_{25})_2]_6$ .

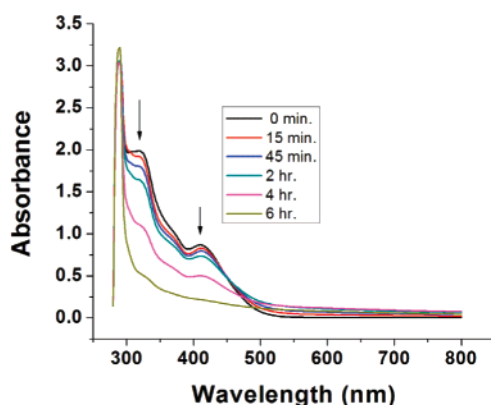


Figure 5. UV/vis spectra of the colloidal solution at different reaction times. The arrows indicate the decrease of the peaks.

3) They are tentatively assigned to ligand-to-metal charge-transfer transition (412 nm), metal-centered transition (320 nm), and ligand-centered transition (272 and 248 nm).<sup>30</sup>

In the IR spectrum of the complex, main peaks are found at 2918, 2849, 1468, and 720  $\text{cm}^{-1}$ , which indicate CH stretching (the first two peaks) modes and CH bending modes (see Supporting Information, Figure S3). In the Raman spectrum, one slightly split peak is found at 345  $\text{cm}^{-1}$ , indicating the Pd–S vibration (see Supporting Information, Figure S4). The powder XRD pattern of the complex reveals it has a more complicated crystalline structure than other layered-structured metal thiolates (see Supporting Information, Figure S5). In the MALDI mass spectrum, the highest peak at 3076.0 is assumed to be the molecular ion peak of  $[\text{Pd}(\text{SC}_{12}\text{H}_{25})_2]_6$  (3053.0) plus  $\text{Na}^+$  ion resulted from the cationizing agent  $\text{CF}_3\text{COONa}$ . The second strongest peak at 2568.0 is assumed to be  $\{[\text{Pd}(\text{SC}_{12}\text{H}_{25})_2]_5\text{Na}\}^+$  (2567.0), a big fragment induced by the ionization. (Figure 4)

**Thermolysis of  $[\text{Pd}(\text{SC}_{12}\text{H}_{25})_2]_6$  in Diphenyl Ether.** The thermolysis of the obtained complex was carried out in diphenyl ether (boiling point 259  $^{\circ}\text{C}$ ) under the protection of argon. At room temperature, the complex was partially dissolved in diphenyl ether under the experimental condi-

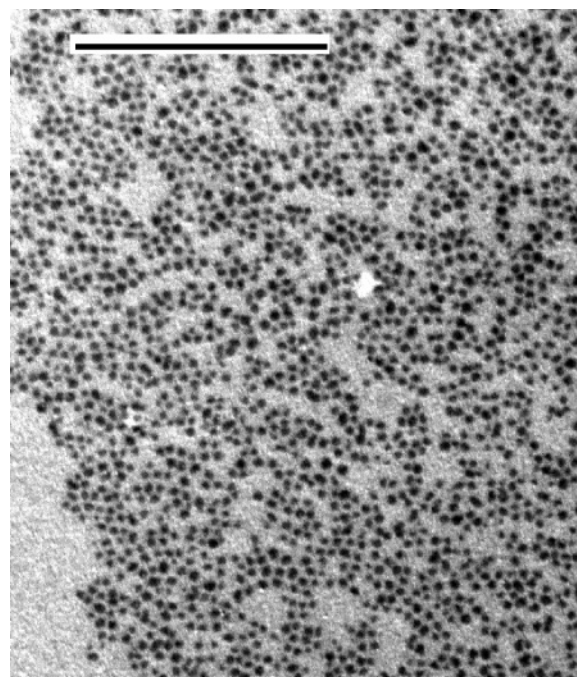


Figure 6. TEM of the obtained nanoparticles after refluxing  $[\text{Pd}(\text{SC}_{12}\text{H}_{25})_2]_6$  for 6 h in diphenyl ether (scale bar = 100 nm).

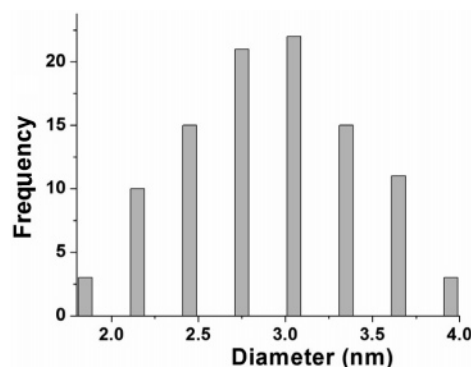


Figure 7. Histogram of the nanoparticles showing the size distribution (diameter =  $2.87 \pm 0.51$  nm, obtained by measuring 100 particles).

tions. When heated, it was totally dissolved and became a clear orange-red solution. At the beginning of reflux, the color of the solution changed to black in 10 min because of the formation of nanoparticles. Then it became darker and darker with longer reaction time. Through tracking the change of the UV spectra, the reaction was found to be complete after 6 h. (Figure 5)

As mentioned before, the complex  $[\text{Pd}(\text{SC}_{12}\text{H}_{25})_2]_6$  has three absorbance peaks (272, 320, 412 nm) in the UV/vis spectrum. Because of the interference of the solvent, the peak at 272 nm is not suitable for the tracking. The other two peaks decrease with reaction time as the complex is gradually transformed to nanoparticles. After 6 h, almost no peaks can be found at these two places and only the scattering effect of the nanoparticles can be observed.

Through TEM analysis, the obtained nanoparticles were found to be spherical, with an average diameter of 2.87 nm and a standard deviation of 0.51 nm (Figure 6 and Figure 7). It is also noticeable that the nanoparticles are well

(30) Tzeng, B. C.; Yeh, H. T.; Huang, Y. C.; Chao, H. Y.; Lee, G. H.; Peng, S. M. *Inorg. Chem.* **2003**, *42*, 6008–6014.

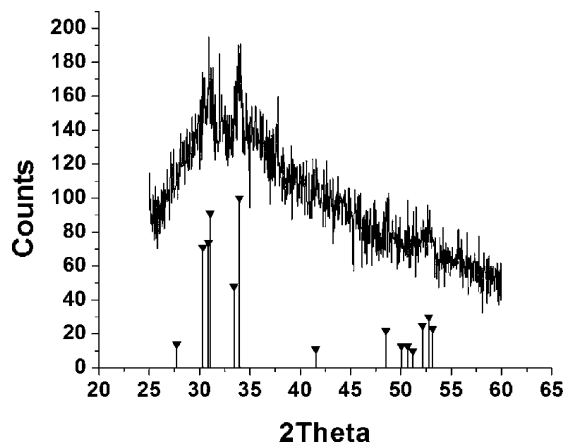


**Figure 8.** Powder XRD pattern of the PdS product obtained by refluxing  $[\text{Pd}(\text{SC}_{12}\text{H}_{25})_2]_6$  for 6 h. The standard PdS pattern is from JCPDS file 25-1234.

separated with an average distance about 2.0 nm, which resembles other monolayer-protected nanoparticles.<sup>31</sup>

The colloidal solution obtained after refluxing was very stable. In a capped vial, it could be kept for months without any color change or sedimentation. It could be washed and separated by polar solvents like ethanol or acetone, and the obtained black precipitates were readily redissolved into nonpolar solvents, such as hexane, toluene, or 4-*tert*-butyltoluene. Elemental analysis of the dry product shows it contains a rather high content of organic species (Pd, 42.6; S, 15.9; C, 29.01; H, 4.79 in wt %), and the molar ratio of Pd to S is about 0.8. Due to the high content of the organic species and the small size of the nanoparticles, the powder XRD analysis shows a rather broad peak with fine features, which indicate the presence of very small PdS crystals (Figure 8).

When the system was refluxed for longer times than 6 h, the nanoparticles gradually aggregated together and precipitated from the solution. A TEM image and an XRD pattern for the sample refluxed for 8 h indicate some aggregated particles and clearer PdS XRD pattern because of the growth of the crystals (see Supporting Information, Figures S6 and S7). It has been found that the aggregation can be prevented by adding additional ligands. For example, when 98  $\mu\text{L}$  of dodecanthiol was injected after 6 h, the system could be refluxed for another 6 h without any appreciable precipitates.

According to all the above-mentioned experimental results, we infer that the obtained product is PdS nanoparticles passivated by a layer of dodecanethiolate species ( $-\text{SC}_{12}\text{H}_{25}$ ), which may be produced when thermolyzing the complex  $[\text{Pd}(\text{SC}_{12}\text{H}_{25})_2]_6$ . Also, the molar ratio of C to H is 2.0 according to the elemental analysis, which is close to 2.1 in  $-\text{SC}_{12}\text{H}_{25}$  species.

## Conclusions

A new tiara Pd(II) thiolate complex,  $[\text{Pd}(\text{SC}_{12}\text{H}_{25})_2]_6$ , was first synthesized with high yield (91.2%) through a simple one-pot reaction, and its structure and properties were further studied by a variety of methods. These results help clarify the reaction system that involves Pd(II) ion and long-chain alkanethiol ligands, which is an usual situation when preparing protected Pd nanoparticles. Also, it gives clues to synthesize other Pd(II) thiolates with long alkyl chains.

Furthermore, nearly monodisperse palladium sulfide nanoparticles ( $2.87 \pm 0.51$  nm) have been synthesized through the thermolysis of the obtained  $[\text{Pd}(\text{SC}_{12}\text{H}_{25})_2]_6$  clusters. The particles were spontaneously passivated by in-situ-formed thiolate species. It will be interesting to study the thermolysis of other Pd(II) alkanethiolates and test the possible influence of chain length of the ligands on the size of the protected nanoparticles.

We believe this sample strategy, i.e., the thermolysis of metal thiolates, can be easily expanded to other metal ions, and now we are investigating the similar methods to prepare metal or metal sulfide nanoparticles of high quality.

**Acknowledgment.** We thank the biology department of Kansas State University for the TEM facilities. Thanks are also given to Dr. John Desper and Dr. Xiao-Min Lin for the help with single-crystal and MALDI analysis.

**Supporting Information Available:** Thin layer chromatography analysis of the room-temperature sample and the refluxed sample; high-temperature  $^1\text{H}$  NMR, IR, Raman, and powder XRD patterns of  $[\text{Pd}(\text{SC}_{12}\text{H}_{25})_2]_6$  clusters; TEM of the sample obtained after refluxing  $[\text{Pd}(\text{SC}_{12}\text{H}_{25})_2]_6$  clusters for 8 h, and the powder XRD of this sample; crystal data and structure refinement of  $[\text{Pd}(\text{SC}_{12}\text{H}_{25})_2]_6$ ; main bond lengths and bond angles of  $[\text{Pd}(\text{SC}_{12}\text{H}_{25})_2]_6$ ; and a CIF file. This material is available free of charge via the Internet at <http://pubs.acs.org>.

IC061242O

(31) Ponce, A. A.; Smetana, A.; Stoeva, S.; Klabunde, K. J.; Sorensen, C. M. *Nanostruct. Adv. Mater.* **2005**, 309–316.